

## Removal of Methylene Blue Dye from Wastewater Using Polydopamine *Agave Americana* Fibres-co-Poly(AAc)/Ag Nanocomposites

Shikha Dogra, Ashvinder Kumar Rana

**How to cite:** Dogra S, Rana AK. Removal of Methylene Blue Dye from Wastewater Using Polydopamine *Agave Americana* Fibres-co-Poly(AAc)/Ag Nanocomposites. Textile & Leather Review. 2023; 6:760-780. <https://doi.org/10.31881/TLR.2023.140>

**How to link:** <https://doi.org/10.31881/TLR.2023.140>

**Published:** 23 November 2023



# Removal of Methylene Blue Dye from Wastewater Using Polydopamine *Agave Americana* Fibres-co-Poly(AAc)/Ag Nanocomposites

**Shikha DOGRA, Ashvinder Kumar RANA\***

Department of Chemistry, Sri Sai University, Palampur, 176061, India

\*ranaashvinder@gmail.com, ranaashvinder2020@gmail.com

## Article

<https://doi.org/10.31881/TLR.2023.140>

Received 13 September 2023; Accepted 13 November 2023; Published 23 November 2023

## ABSTRACT

*In this research, efforts have been made to tailor the surface of Agave americana fibre by utilising a sequence of chemical techniques and their subsequent utilisation as adsorbents to remove methylene blue dye from wastewater. The surface modification of Agave americana cellulosic fibre was carried out by utilising a polydopamine (PDA) coating agent, which was subsequently graft copolymerized with vinyl monomer acrylic acid (AAc), and finally doped with silver nanoparticles (Ag NPs) to synthesise nanocomposites. Different characterisation techniques, such as SEM, FTIR and XRD were used to characterise the samples and UV-visible spectroscopy was utilised to assess their potential for the removal of dye from wastewater. The grafting of polydopamine, polyacrylic acid, and silver nanoparticles onto the cellulosic fibre resulted in morphological changes and the formation of new bonds, as confirmed by SEM images and FTIR spectra of the grafted samples, respectively. Further, during the dye adsorption/degradation study, among different surface-modified fibres, silver nanoparticles-doped Agave americana fibres graft copolymerized samples showed a maximum of 94.40% dye adsorption/degradation tendency and 85.20 mg/g adsorption capacity. Further, the adsorption was found to be close to Langmuir adsorption.*

## KEYWORDS

*methylene blue, wastewater, polydopamine, Agave americana, acrylic acid, silver nanoparticle, adsorption*

## INTRODUCTION

Water is a vital renewable resource for all forms of life, including economic development, food production and normal well-being. The dyes emitted from textile pigment and leather industries are one of the biggest causes of water pollution. Since, through drinking water, it enters the food chain and thus may lead to major health problems such as carcinogenicity and mutagenesis [1]. Numerous techniques have been employed for treating drinkable water, including physiochemical, reverse osmosis, electrochemical, membrane, electrodialysis, advanced oxidation, ion exchange and adsorption methods [2–5]. However, the majority of these technologies produce harmful chemicals and are expensive to operate and maintain. Among different techniques, adsorption is the most efficient, affordable and popular, which can be carried out by utilizing low-

cost adsorbents like bio-based/natural and agricultural-based materials [6].

Recently, different biological materials i.e., chitin, chitosan, yeast, and fungal biomass, have been used in the adsorption of dyes from solutions, which typically occurs through chelation and composition mechanisms [7]. However, among different adsorbing materials, bio-mass-based adsorbents have received a lot of attention because of their low cost, eco-friendliness and easy availability [8–10].

The potential of agricultural and plant wastes for the adsorption of dyes has been explored by numerous researchers [11,12]. Various adsorbents such as ash, straw, plant leaves, fruit peels, plant bark, etc., have been explored. Further, to enhance their adsorption potential, surface modification may be an alluring technique and has been preferred by several researchers [13–16]. Dye adsorption tendencies of biomass have been observed to depend upon the type of materials used, surface modification techniques employed and nature of the dyes [15,17].

Cellulosic fibres or natural fibres derived from agricultural wastes or wood biomass, comprise three major polymers, namely cellulose, hemicelluloses and lignin [18,19]. Each of the constituents displays specific properties and plays a key role in the adsorption of dyes through interaction (hydrogen bonding, van der Waals interactions, ionic and covalent bonds) between specific functional groups (OH, COOH or other functional groups created after the surface modification) presented onto virgin cellulosic biomass or surface modified biomass with dyes [15,18,20].

A total of  $7 \times 10^5$  t of commercial dyes, including acidic, basic, direct, pigment dyes, etc., are produced each year [21]. Among these dyes, basic dye (a cationic dye that contains positively charged sulphur or nitrogen atoms) has been categorized as a hazardous colourant, because it produces colouration even at extremely low concentrations (less than 1 mg/L) [22]. Basic methylene blue (MB) dye has been used as a dyeing agent in a variety of industrial applications, including leather, calico, cotton, and tannins as well as a biological staining agent [23]. Acute exposure to this dye may cause various health problems such as cyanosis, convulsions, methaemoglobinaemia, gastrointestinal problems, ocular discomfort, and dyspnea [24].

AAFs, either in their raw state or after blending/surface modification, have been used in a wide range of applications. These applications include the adsorption of heavy metals such as Cd (II) and Pb(II) [25,26], phytoremediation of soil contaminated with cadmium [27], reinforcing the TiO<sub>2</sub>/polyester resin-based composites [28] and adsorption of dyes i.e., MB [29], malachite green [30], sumfixe supra red [31], alpacelle lumiere brown [31] and alpacide yellow [32]. Gupta et al. [33] grafted *Luffa* cylindrical fibre and *Ficus carica* fibre [34], Sharma et al. [35] grafted *Hibiscus cannabinus* fibre, Pomicipic et al. [36] grafted pineapple leaf fibre and Hakram et al. [37] grafted bacterial cellulose with acrylic acid (AAc) for adsorption of MB dye from wastewater and reported that AAc graft copolymerization significantly impacts the adsorbing nature of biomass. Hamissa et al. used raw AAF fibres for the adsorption of methylene blue, but in the present study, we have modified the surface of

pretreated AAFs by bio-compatible dopamine followed by polyacrylic acid and finally doped the obtained materials with the silver nanoparticle to enhance its MB adsorption or degradation tendencies [29]. We have preferred dopamine grafting onto AAFs because of its biocompatible nature and no one has yet explored the adsorbing nature of the combined impact of dopamine/ AAC/ Ag nano particles for adsorbing dyes.

## EXPERIMENTAL

### Materials

Raw AAFs were extracted from the leaves of *Agave americana* plants through water water-retting process and subsequently cleaned and purified before their surface modification. Further, dopamine (3, 4-dihydroxyphenethylamine hydrochloride, Molecular formula-  $C_8H_{11}NO_2$ ) of SIGMA made, AAC supplied from CDH, sodium hydroxide from Union Drug & Chemical Company, India, nitric acid from Qualigens, India, ceric ammonium nitrate from OXFORD LAB FINE CHEM LLP, made and  $(NH_4)_4Ce(SO_4)_4$  and silver nitrate from Fisher Scientific, made and MB dye supplied from Alpha Chemika, India were utilized in the present research work.

### Experimental section

#### *Pretreatment of raw AAFs*

The raw fibres were washed in a 2% detergent solution and subsequently cleansed with distilled water and dried. The dried fibres were chopped into lengths of 5-8 mm. The short fibres were then treated for 210 minutes at room temperature with a 10% (w/v) NaOH solution to remove waxes and other soluble contaminants. The treated fibres were then rinsed with distilled water and subsequently dried in a hot air oven.

#### *Synthesis of AAFs-grafted-Polydopamine (AAFs-g-PDA) fibres*

For the synthesis of PDA-doped AAFs, 4 g of pretreated fibres were immersed in 500 mL of distilled water and stirred vigorously for 15 minutes. Afterwards, the pH of the solution was maintained at 8.5 with the help of tris buffer solution. In the next step, 2.0 g of dopamine was added to the above-prepared suspension and stirred magnetically for 24 hours at room temperature. During the polymerization process, the colour of the resultant dispersion slowly turned black. Finally, the grafted product was rinsed 2-3 times with deionized water and subsequently dried in a hot air oven at 60 °C.

### *Synthesis of AAFs-g-PDA + Poly (AAc) graft copolymer*

2 gm of AAFs-g-PDA cellulosic polymer fibres were soaked in 100 mL of distilled water for 24 hours before the grafting process. A known quantity of the initiator system, i.e., 0.5 g ceric ammonium nitrate (CAN) and nitric acid ( $2.77 \times 10^{-1}$  mol/L) was added to the reaction mixture to initiate graft copolymerization. Further, 2 mL of AAc (monomer) was added to the reaction mixture with constant stirring. The resulting mixture was then stirred continuously for 90 min while maintaining the reaction temperature at 45 °C. The grafted fibres were then carefully washed with distilled water and dried at 60 °C in a hot air oven.

### *Synthesis of AAFs-g-PDA+ Poly (AAc) +AgNPs doped composites*

For doping of silver particles, 1 gm of AAFs-g-PDA+ Poly (AAc) dried fibres were immersed and stirred constantly in an  $\text{AgNO}_3$  (500 ml) solution for 1 hr. The reaction mixture was then allowed to stand for 20 min in a water bath and subsequently treated with 10 mM NaOH or  $\text{NaBH}_4$  solutions to reduce silver ions into nanoparticles. Afterwards, the NP-impregnated cellulosic fibres were rinsed in ethanol and deionized water to eliminate any remaining unbound NPs. The synthesised material was dried overnight and then in a hot air oven at 60 °C. The procedure as reported in this section was utilised for the synthesis of AAFs-g-PDA-AgNPs.

### *Evaluation of the dye absorption behaviour of synthesised samples*

To evaluate the absorption behaviour, a dye solution was prepared by dissolving 1.5 g of powdered MB dye in 100 ml of 95% (v/v) ethyl alcohol solution. Further, 30 ml of the prepared dye solution was diluted with 100 mL of distilled water and subsequently with a 10% KOH solution. Finally, 0.5 mg of each grafted fibre sample was added to 100 ml of basified dye solution (pH:9) of a specific concentration, i.e., 10, 20 and 30 mg/L and stirred vigorously for 1 hour at room temperature (15 °C). The samples after being dipped in dye solutions were filtered out and their dye absorption behaviour was studied using the UV technique.

### *Characterization techniques*

Scanning electron microscopy (SEM) study of different samples was performed using the Nova Nano SEM-450 model made by JFEI company of USA (S.E.A.) PTE LTD. All samples were coated with gold before focusing the electron beam. Fourier-transform infrared spectroscopy (FTIR) study of different samples was carried out in a spectrum PE IR Subtech Spectrum ASCII PEDS instrument by using KBr in the range  $4,000-400 \text{ cm}^{-1}$ . Further, a crystallinity study was done on the SmartLab 9 kW rotating anode x-ray diffractometer model of Rigaku Corporation. The studies were carried out using a Ni-filter,  $\text{Cu K}\alpha$  radiation and a scintillation counter as a detector at 40 kV on rotation from  $10^\circ$  to  $80^\circ$  at  $2\theta$  scale. The

dye adsorption capability of samples was determined by measuring absorbance at 665 nm utilising a double-beam UV–vis spectrophotometer made by Systersonics, model 2202.

## RESULTS AND DISCUSSION

### Surface modification of *Agave americana* fibres

Natural fibres are generally modified to enhance their dye and heavy metal adsorption properties. The reaction mechanism for the synthesis of AAFs-g-PDA fibres [38] or AAFs-g-PDA-poly(AAc) [39] and AAFs-g-PDA-poly(AAc)/Ag nanocomposites has been given in Figures 1, 2 and 3. The doping of polydopamine onto AAFs was carried out in a basic medium as illustrated below (Figure 1).

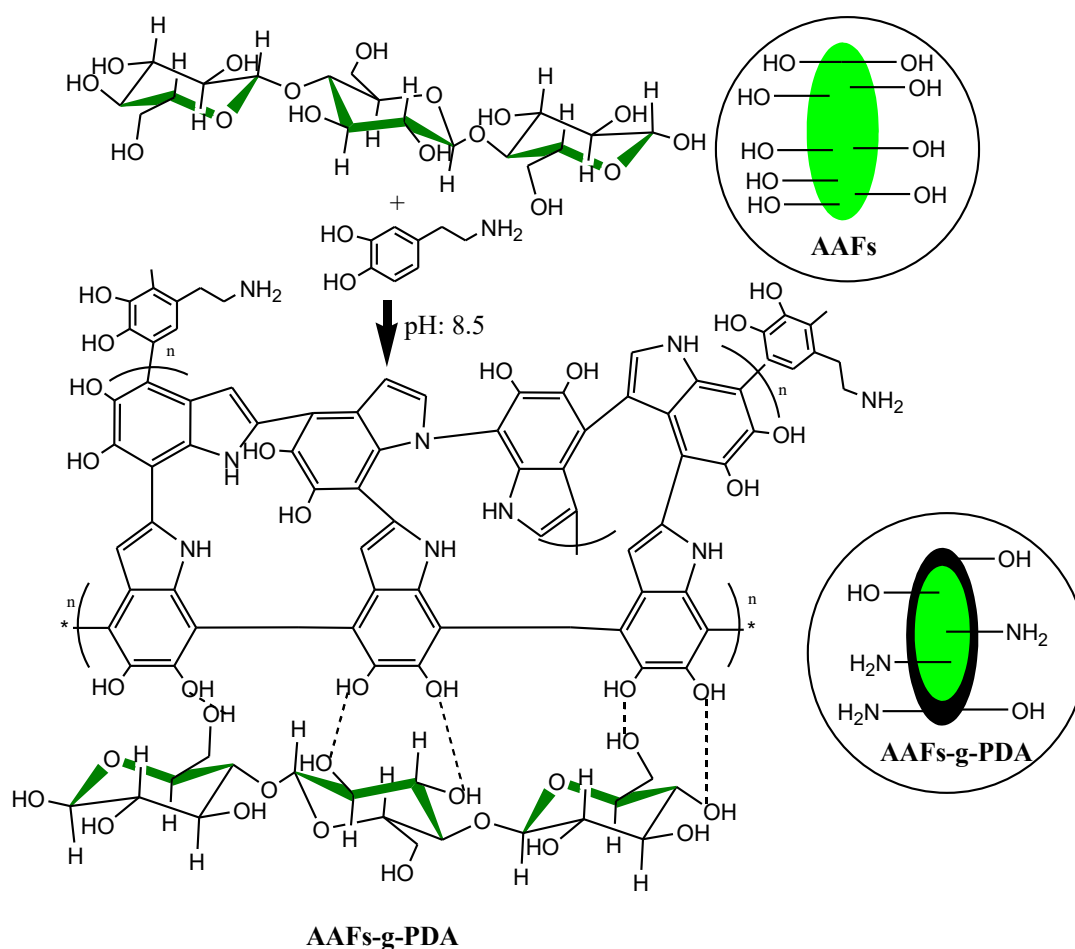


Figure 1. Reaction mechanism for synthesis of AAFs-g-PDA[38]

The free hydroxyl groups on cellulosic fibres and PDA chains may serve as an active site for graft copolymerization of AAc polymeric chains (Figure 2). Through the C<sub>2</sub> and C<sub>3</sub> -OH groups in AAFs or hydroxyl/amine groups in the PDA chain, ceric ions from CAN may form a chelate complex with the cellulose molecule or PDA molecules. The transfer of an electron from the cellulose molecule or grafted

acrylic acid reduces  $Ce^{4+}$  to  $Ce^{3+}$ . The following mechanism is thought to be involved in the grafting of AAc onto the backbone [40].

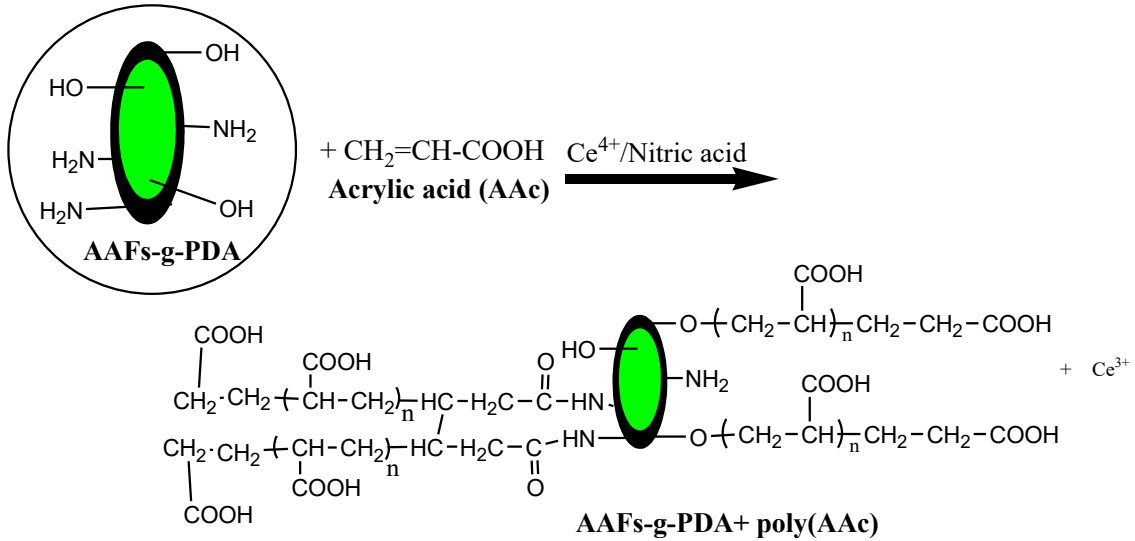


Figure 2. Showing the possible outcome after graft copolymerization of AAc onto AAFs-g-PDA fibre [39]

The ceric ions form complexes with the carbon chains of AAFs doped with PDA, resulting in free radicals. Similarly, ceric ions also create free radicals in monomer chains, which then attach to the active site on the polymer backbone to form the graft copolymer. The various monomer free radicals may combine to form the homopolymer. Further, the reaction scheme for the synthesis of AAFs-g-PDA+ Poly (AAc)+ AgNPs/ AAFs-g- PDA+ Ag nanocomposites has been given in Figure 3.

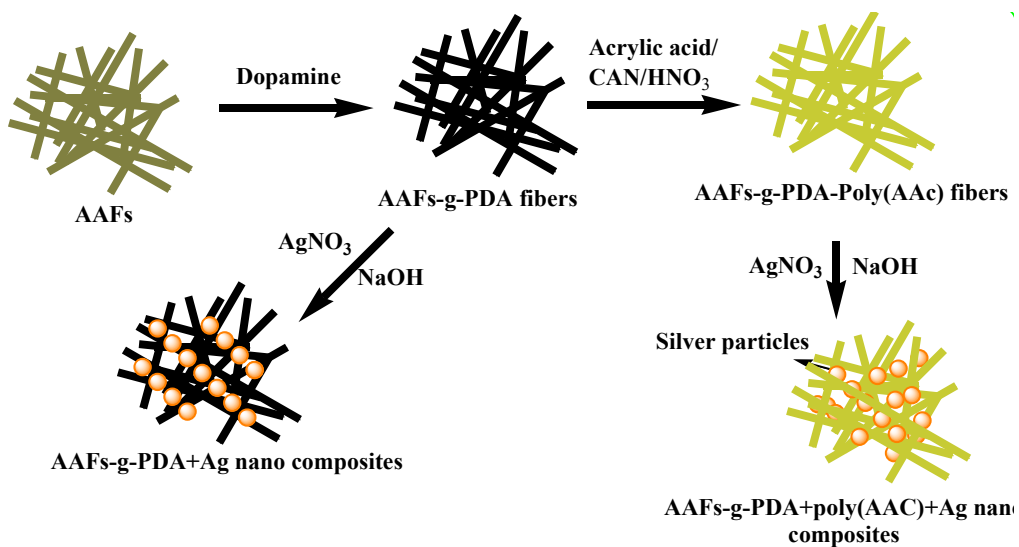


Figure 3. Schematic illustration for graft co-polymerization of AAFs-g-PDA+ Poly (AAc) +Ag nanocomposites and AAFs-g-PDA+ Ag nanocomposites

### Scanning electron microscopy

The SEM technique is used to investigate changes in the morphology of fibre surfaces. The SEM of pretreated AAFs, AAFs-g-PDA, AAFs-g-PDA+ Poly (AAc) graft copolymer, AAFs-g-PDA+ Poly (AAc)+ AgNPs doped nanocomposites and AAFs-g-PDA+ Ag NPs doped nanocomposites are shown in Figure 4a, b, c, d and e. From Figure 4a, it has been noticed that AAFs are cylindrical and contain a parallel set of microfibrils. On comparing figures 4 (a) and (b), it has been noted that there are no major changes in the morphology of the AAFs after PDA doping; however, the surface of the fibres becomes smoother after doping PDA onto the AAFs surface.

Further, upon grafting poly (AAc) onto AAFs-g-PDA, a large amount of AAc has been observed to be deposited on the fibre backbone, causing many morphological alterations in the fibre (Figure 4c). Also, after grafting with AAc, the fibre surface became more rough and uneven [41]. The roughness of fibres was further noticed to be enhanced after the deposition of spherical-polydisperse silver nanoparticles onto AAFs-g-PDA-poly (AAc) (Figure 4(d)). In comparison to the pretreated fibre, AAFs displayed in figure 4c and d, are quite rough because of the high graft density and thus may lead to strong adhesion with hydrophobic thermosetting/thermoplastic matrices [42]. From Figure 4e, we can also notice the deposition of silver nanoparticles onto the AAFs-g-PDA surface since the fibre becomes rougher when compared with AAFs-g-PDA fibre.

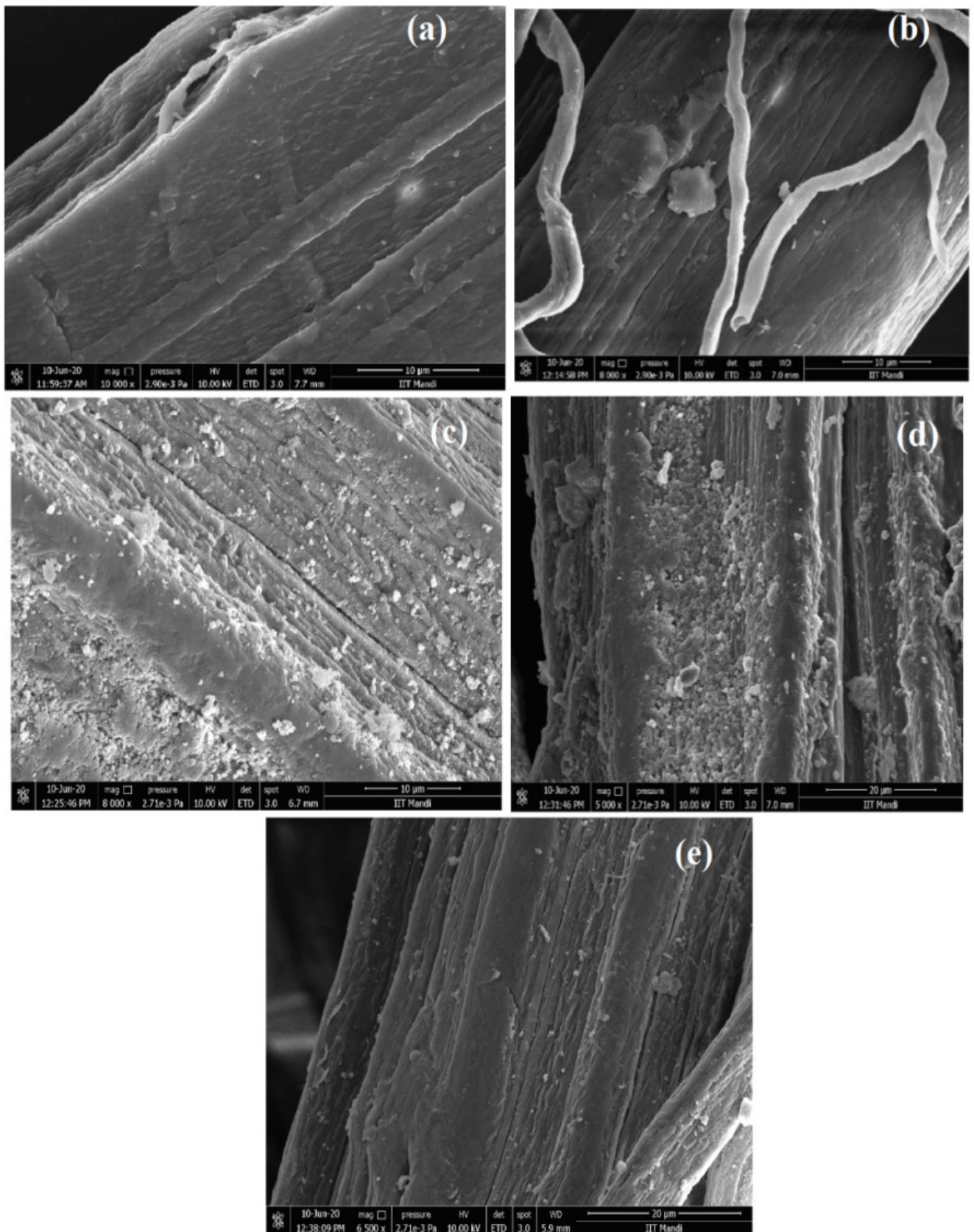


Figure 4. Scanning electron micrograph of (a) Pretreated AAFs (b) AAFs-g-PDA fibre (c) AAFs-g-PDA+Poly (AAc) graft copolymer (d) AAFs-g-PDA+ Poly (AAc) + AgNPs doped composites and (e) AAF-g-PDA + AgNP doped composites

## FT-IR Analysis

FTIR spectral analysis of pretreated AAFs, AAFs-g-PDA, AAFs-g-PDA+Poly (AAc) graft copolymer, AAFs-g-PDA+ Poly (AAc) + AgNPs doped nanocomposites and AAFs-g-PDA + AgNPs doped nanocomposites is given in Figure 5. In the FTIR spectra of pristine AAFs, a prominent peak at  $3393\text{ cm}^{-1}$  because of stretching of the bonded hydroxyl group (-OH), present on AAFs was observed [39]. The broadness of this peak might be because of the inter- and intra-molecular hydrogen bond vibrations. Further, due to asymmetric and symmetric C-H stretching of the  $\text{CH}_2$  group, absorption peaks at  $2938\text{ cm}^{-1}$  and  $2853\text{ cm}^{-1}$ , respectively, were also confirmed. Peaks at  $1385$ ,  $1412$ , and  $1482\text{ cm}^{-1}$  could be attributable to the bending of -CH,  $-\text{CH}_2$ , and  $-\text{CH}_3$ , respectively. The other absorption peak,  $744\text{ cm}^{-1}$ , could be due to  $\beta$ -glycosidic linkage and C-C stretching vibration, while at  $642\text{ cm}^{-1}$  could be due to out-of-plane hydroxyl (-OH) bending.

Upon grafting with PDA, some major absorption bands are detected in the spectrum, as shown in Figure 5. A strong and wide absorption band at  $3389\text{ cm}^{-1}$ , aroused due to the O-H stretching vibration, confirms the presence of the cellulose backbone. In addition to other conventional vibrational peaks, as observed in the case of pristine AAFs, a medium-strong absorption peak at  $1529\text{ cm}^{-1}$  because of the N-H bending vibration has been observed, which may confirm the doping of PDA onto the fibre's surface. Further, no additional peak, in the case of AAFs-g-PDA fibres, for  $-\text{CO}$  stretching (present in phenolic moieties), -N-H vibration or indole ring stretching vibration, which are the characteristics peaks for PDA, were observed at  $1274$ ,  $1510$  and  $1600\text{ cm}^{-1}$ , respectively. This might be because of the presence of cellulose, hemicelluloses and lignin in the AAF backbone, which possess almost similar functional groups as those of PDA and thus may overshadow the peaks of PDA.

In the FTIR spectra of the AAFs-g-PDA+ Poly(AAc) graft copolymer, some additional changes are noted in the absorption peaks of spectra. An increase in the intensity of the peak at  $1574\text{ cm}^{-1}$  due to the unsaturated group and a peak at  $1733\text{ cm}^{-1}$  due to the carbonyl stretching of the COOH group of polyacrylic acid chains were observed. The presence of new additional absorption peaks confirmed the successful grafting of poly (AAc) chains onto AAFs-g-PDA [43].

In the FTIR spectra of AAFs-g-PDA+ Poly(AAc)+ AgNP doped composites, no change in the absorption peaks, when compared to AAFs-g-PDA+ Poly(AAc) fibres, was observed. A strong broad absorption band at  $3403\text{ cm}^{-1}$ , due to the presence of O-H stretching vibration, a medium-strong band at  $1657\text{ cm}^{-1}$  due to carbonyl stretching of (NH)C=O group and a mild band at  $1386\text{ cm}^{-1}$  because of the presence of N-O symmetric stretching have been observed. From Figure, we can observe that both AAFs-g-PDA+ Poly(AAc) fibres and AAFs-g-PDA+ Poly(AAc) + Ag nanocomposites display almost the same peaks (FTIR spectra). This confirms that Ag metal in nanocomposites is present in its metallic form (a potential metal-organic form of silver metal is absent here). Also, the absence of peaks at  $1120\text{ cm}^{-1}$  and  $1398$

$\text{cm}^{-1}$ , which generally arise because of metal–OH and metal–oxygen bonds, further confirms the existence of metallic forms of Ag metals [44].

In the FTIR spectra of AAFs-g-PDA+ AgNPs doped composites, no additional peak, when compared with AAFs-g-PDA fibres, was observed. Further, the metallic doping of Ag nanoparticles onto doped fibres can be assigned in the same manner as discussed in the previous paragraph.

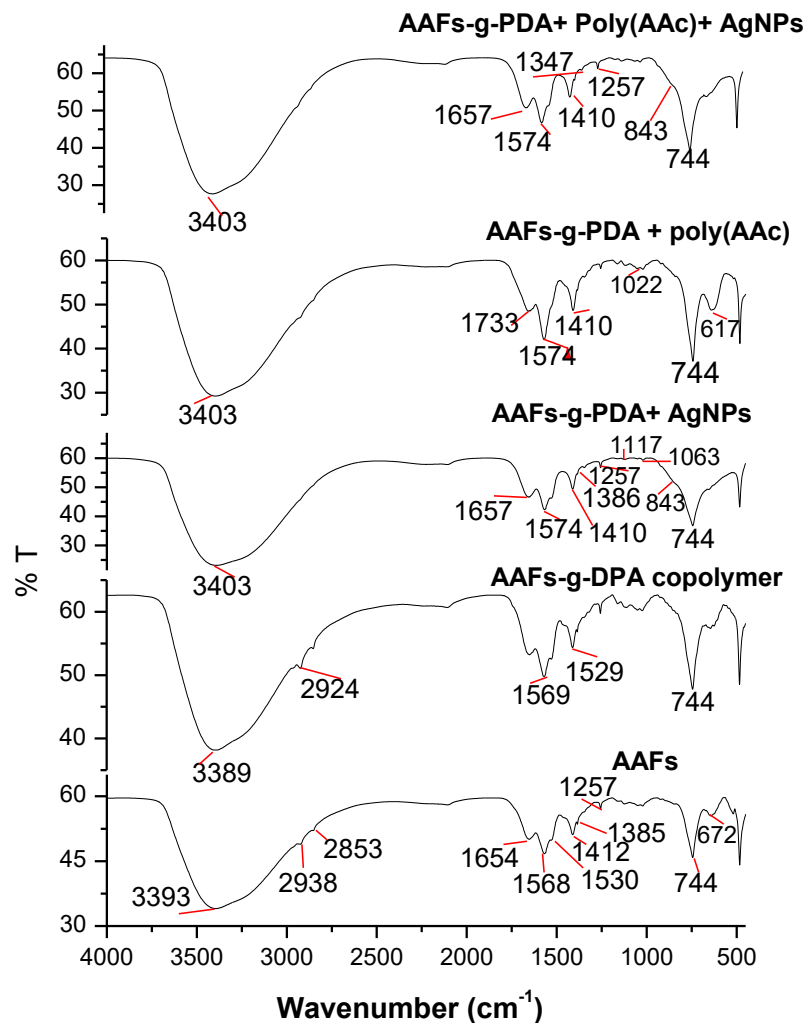


Figure 5. FTIR spectra of pretreated and different surface functionalized fibres

### XRD studies

Figure 6 depicts the XRD patterns of pretreated AAFs, AAFs-g-PDA co-polymer, AAFs-g-PDA+ Poly (AAc) graft copolymer, AAFs-g-PDA+ Poly (AAc) + AgNPs doped nanocomposites, and AAFs-g-PDA+ AgNPs doped nanocomposites. The primary broad and dispersed characteristic peaks in pretreated AAFs have been detected at  $22.05^\circ$  and  $14.20^\circ$ , respectively, with relative intensities of 1320 and 681, respectively, indicating the amorphous nature of AAFs [45]. In the case of the AAFs-g-PDA co-polymer, the distinctive peaks have been found at  $16.14^\circ$  and  $23.06^\circ$ , with relative intensities of 2171 and 811, respectively. The characteristic peaks of the AAFs-g-PDA+ Poly (AAc) graft copolymer, on the other

hand, have been found at 22.16° and 16.40°, respectively, with lower relative intensities of 476 and 352, indicating that Poly (AAc) chains were grafted onto the cellulose backbone through covalent bonding. As a result, upon grafting, the percentage of crystallinity falls as stiffness and toughness decrease [39,42]. The crystallinity index (C.I.) and the proportion of crystallinity (% X<sub>c</sub>) are calculated as follows:

$$C.I. = \frac{I_C - I_A}{I_C} \quad (1)$$

$$\% X_C = \frac{I_C}{I_A + I_C} \times 100\% \quad (2)$$

where I<sub>A</sub> is the amorphous phase's peak intensity and I<sub>C</sub> is the crystalline phase's peak intensity.

The C.I of pretreated AAFs, AAFs-g-PDA, AAFs-g-PDA + Poly (AAc) graft copolymer, AAFs-g-PDA + Poly (AAc) + Ag nanocomposites and AAFs-g-PDA + Ag nanocomposites was observed as 0.48, 0.62, 0.26, 0.59 and 0.50, while the % X<sub>c</sub> was calculated to be 65.80, 72.80, 57.80, 74.80 and 66.80%, respectively. On doping of AAFs with PDA, an increase in % X<sub>c</sub> was observed, while a considerable decrease in % X<sub>c</sub> after graft copolymerization of AAc onto AAFs-g-PDA fibre was noticed. The decrease in crystallinity of the AAFs-g-PDA + Poly (Aac) graft copolymer may be because of an increase in disorder or randomness in the crystal lattice of cellulosic fibre (Table 1) after the inclusion of Poly (AAc) chains on the active site of the backbone during grafting, resulting in more amorphous cellulosic fibre.

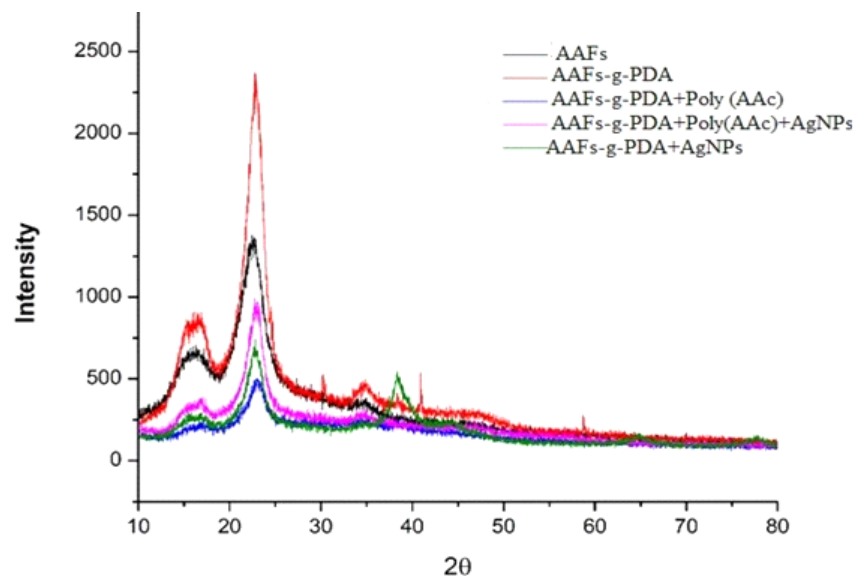


Figure 6. XRD pattern of pretreated AAFs and other grafted samples

Further, in case of AAFs-g-PDA+ Poly (AAc) + AgNPs and AAFs-g-PDA + AgNPs doped nanocomposites the intense characteristic peaks, which correspond to the (1 1 1), (2 0 0) and (2 2 0) diffraction planes of silver nanoparticles, appeared at 38.12°, 44.14°, 64.08° and 39.02°, 45.03°, 65.12° and 78.1°,

respectively. The peaks were found to be reliable with the database in JCPDS card no. 75-576 and results confirm the presence of a face-centred cubic crystal structure of silver nanoparticles [46,47]. The XRD results disclose the successful deposition of AgNPs on the surface of AAFs. The average crystalline size of AgNPs was calculated by the Debye Scherrer equation as given below.

$$(D = K\lambda/\beta\cos\theta) \quad (3)$$

Here, D, K,  $\lambda$ ,  $\beta$  and  $\theta$  represent the nanoparticle size, a constant (0.89), X-ray wavelength (1.54 Å), full-width half maximum (FWHM) and half diffraction angle, respectively. The average crystalline size of AgNPs, calculated by using the above equation, is estimated to be 11.5 nm. These results were found to be reliable with the findings of other researchers [47–49].

### Removal of MB dye from aqueous medium

One of the most convenient characterization techniques for determining dye removal efficiency is UV-visible spectroscopy. The initial concentration of MB dye was varied and its impacts on pretreated AAFs and other synthesised samples were investigated. The effect of initial MB dye concentrations (10, 20 and 30 mg/L) on % dye removal efficiency of different AAFs grafted samples was examined at room temperature (35 °C) for a fixed time of 1 hr. The results are shown in Table 2. The final/equilibrium dye concentration ( $C_e$ ) was measured for pretreated AAFs as well as other grafted samples and the percentage dye removal and adsorption capacity were calculated using the following relationships:

$$\% \text{ Dye removal} = (C_i - C_e) / C_i \times 100 \quad (4)$$

$$\text{Adsorption capacity } (q_e) = (C_i - C_e) * V / M \quad (5)$$

On comparing the results, it has been noticed that the % dye removal efficiency is highest in the case of AAFs-g-PDA+Poly (AAc) + Ag nanocomposites followed by AAFs-g-PDA+ Ag nanocomposites, AAFs-g-PDA+Poly (AAc) fibres, AAFs-g-PDA and pretreated AAFs fibres (Figure 7). The better dye removal efficiency in the case of silver nano particles-doped samples (AAFs-g-PDA+Poly (AAc) + Ag and AAFs-g-PDA+ Ag nanocomposites) might be because of the adsorbing as well as reductive nature of silver nanoparticles doped cellulose backbone samples (Figure 8). Further, maximum adsorption capacity (83.97 mg/g) was observed for AAFs-g-PDA+Poly (AAc) + Ag at a dye concentration of 30 mg/l; while a minimum (21.6 mg/g) was found for pretreated AAFs at 10 mg/l dye concentration. However, higher adsorption in the case of the AAFs-g-PDA+Poly (AAc) + Ag sample might be due to synergistic effects of dye degradation as well as adsorption. Upon plotting the graph between  $C_e/q_e$  and  $C_e$  [using

equation 7, linear form of Langmuir adsorption model (equation 6)), the correlation coefficients for all samples were found to be close to 1 (Table 2), which indicates that the adsorption of MB onto adsorbing materials fits the Langmuir adsorption [50]. It confirms that the adsorbent surface is homogeneous and that adsorbate is adsorbed as a monolayer on it.

$$\text{Langmuir adsorption model: } q_e = \frac{Q_0 K_L C_e}{1 + K_L C_e} \quad (6)$$

$$\text{Linear form: } \frac{C_e}{q_e} = \frac{1}{K_L Q_0} + \frac{C_e}{Q_0} \quad (7)$$

Here ' $K_L$ ' is the Langmuir adsorption equilibrium constant and  $Q_0$  is the maximum amount of the dyes adsorbed per unit weight of the adsorbent (mg/g).

The dye removal efficiencies were noticed to decline from 94.4% to 90.0% when the initial MB concentration was increased from 10 to 30 mg/L, which might be because of blockage of all adsorbing sites or the unavailability of sufficient catalytic amounts of the silver nanoparticles onto backbone fibres. Further, the improvement in the per cent dye removal efficiency of AAFs after their surface modification with PDA and AAc has been attributed to the better adsorbing nature of PDA and poly(AAc) chains towards MB. It has also been noticed that among AAFs-g-PDA+Poly (AAc) + Ag and AAFs-g-PDA+ Ag nanocomposites, the former showed higher dye removal efficiency. This behaviour might be because of the higher adsorption and silver ions take-up capacity of AAFs-g-PDA+Poly (AAc) samples than AAFs-g-PDA fibres [49]. So, our study concludes that AAFs-g-PDA+ Poly (AAc)+ Ag nanocomposites are promising adsorbents for removing MB dye from aqueous solutions.

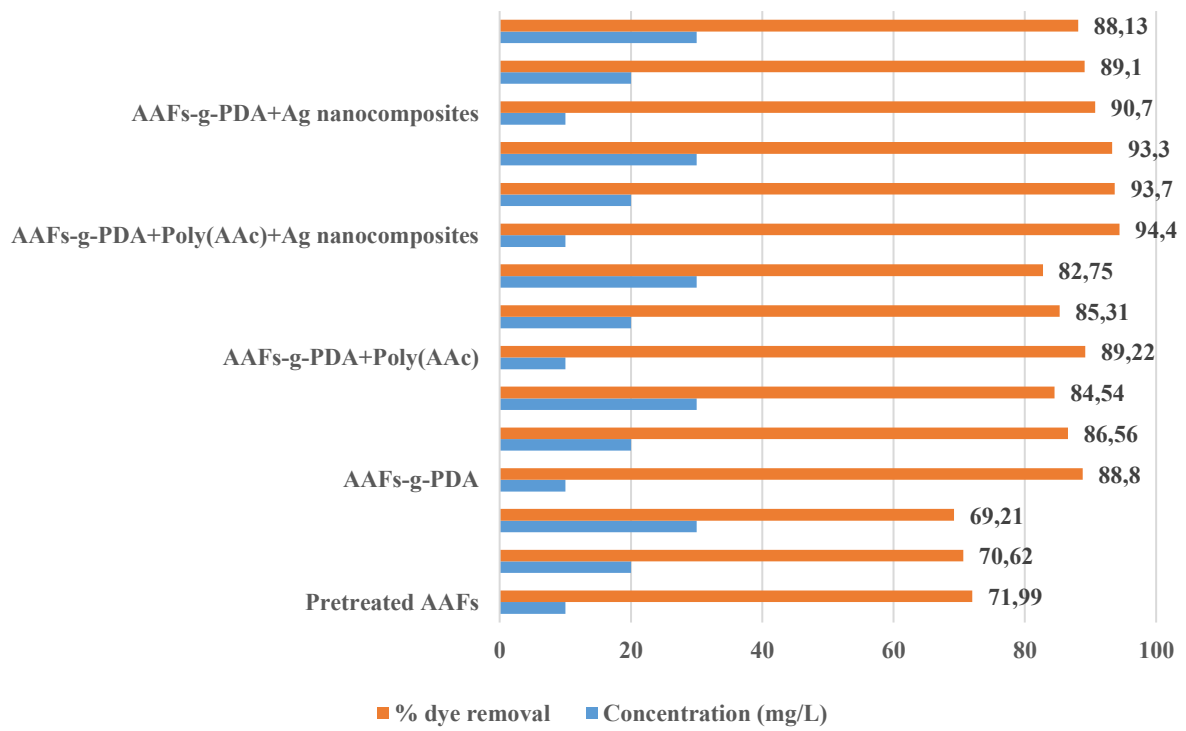


Figure 7. % MB dye removal capability of different adsorbents

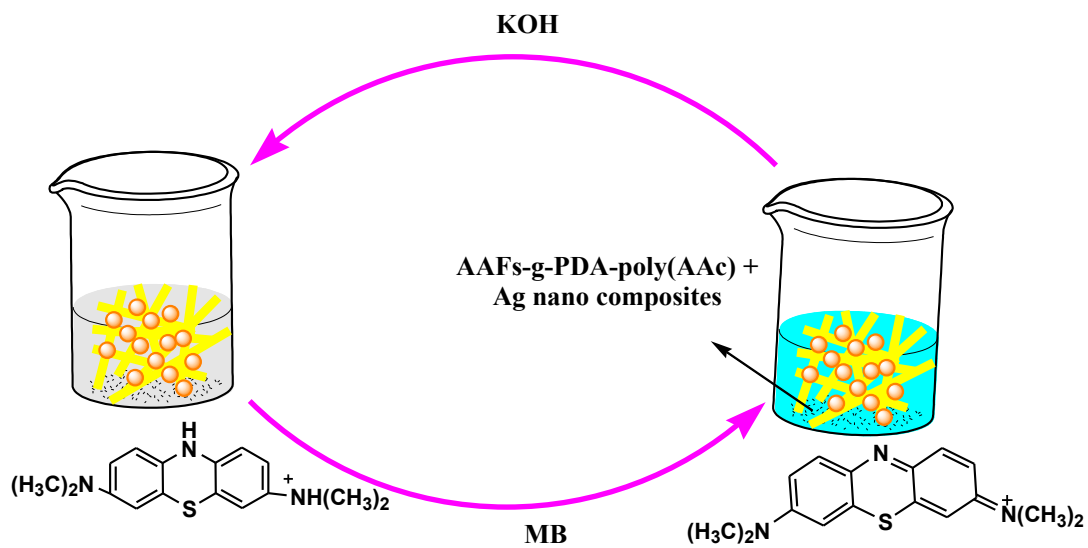


Figure 8. Showing the reduction of MB dye after the addition of AAFs-g-PDA + poly (AAc) + Ag nanocomposites in dye solution

Table 1. Crystallinity index and Percentage crystallinity of pretreated AAFs and other grafted samples

Samples	2θ		Intensity			%XC
	Crystalline peak	Amorphous peak	IC	IA	C.I.	
PretreatedAAFs	22.05	14.20	1320	681	0.48	65.80
AAFs-g-PDA	23.06	16.14	2171	811	0.62	72.80

Samples	2 $\theta$		Intensity		C.I.	%XC
	Crystalline	Amorphous	IC	IA		
	peak	peak				
AAFs-g-PDA +Poly (AAc)	22.16	16.40	476	352	0.26	57.80
AAFs-g-PDA +Poly (AAc)+ Ag nanocomposites	38.12	16.14	821	332	0.59	74.80
AAFs-g-PDA+Ag nanocomposites	45.03	16.12	623	311	0.50	66.80

Table 2. Comparison of % MB dye removal between pretreated AAFs and other grafted samples

Samples	Initial dye concentration (Ci)	Equilibrium dye concentration (Ce)	Absorbance	Adsorption capacity (qe: mg/g)	% Dye removal	Coefficient of correlation as per Langmuir isotherm
Blank dye solution	10	-	0.215	-	-	
	20	-	0.240	-	-	
	30	-	0.338	-	-	
Pretreated AAFs	10	2.8	0.06	21.6	71.99	0.992
	20	5.88	0.07	42.36	70.62	
	30	9.14	0.08	62.58	69.21	
AAFs-g-PDA	10	1.21	0.024	26.37	88.80	0.996
	20	2.68	0.032	51.96	86.56	
	30	4.64	0.052	76.08	84.54	
AAFs-g-PDA+Poly(AAc)	10	1.07	0.026	26.79	89.22	0.975
	20	2.94	0.035	51.18	85.31	
	30	5.17	0.058	74.49	82.75	
AAFs-g-PDA+Poly(AAc)+Ag nanocomposites	10	0.56	0.012	28.32	94.40	0.970
	20	1.26	0.015	56.22	93.70	
	30	2.01	0.018	85.2	93.30	
AAFs-g-PDA+Ag nanocomposites	10	0.93	0.022	27.21	90.7	0.965
	20	2.18	0.020	53.46	89.1	
	30	3.56	0.024	79.32	88.13	

## CONCLUSION

Graft copolymerization is one of the most attractive methods for tailoring the characteristics of natural fibre. In the present study, PDA, vinyl monomer Poly (AAc), and Ag nanoparticles have been successfully grafted onto AAF cellulosic fibre, sequentially. Different techniques, such as SEM, FTIR, XRD, and UV-Vis. spectroscopy was used to characterize the pretreated AAFs and other grafted samples. The improved surface morphology after the grafting was confirmed by SEM technique. The FTIR results of grafted fibres showed the presence of new adsorption peaks for synthesized samples. In the case of AAFs-g-PDA + Poly (AAc) + Ag nanocomposites, no change in the adsorption peak was absorbed when compared to AAFs-g-PDA + Poly (AAc) fibres. This confirms that Ag metal

in nanocomposites is present in its metallic form. XRD pattern showed the diffraction peaks at  $23.12^\circ$  and  $23.11^\circ$  which support the formation of silver nanoparticles with FCC structure. UV-Vis. results showed the impact of initial MB dye concentrations on the adsorbing nature of pretreated AAFs and other grafted samples. The % dye removal efficiency of AAFs-g-PDA + Poly (AAc) + Ag nanocomposites had been found better as compared to other grafted samples. Thus, the AAFs-g-PDA + Poly (AAc) + AgNPs doped composites may serve as a promising adsorbent for the removal of MB dye from an aqueous solution.

#### *Author Contributions*

Conceptualization – Dogra S, Rana AK; methodology – Dogra S, Rana AK; formal analysis – Dogra S; investigation, resources; writing-original draft preparation – Dogra S; writing-review and editing – Rana AK. All authors have read and agreed to the published version of the manuscript.

#### *Conflicts of Interest*

The authors declare no conflict of interest.

#### *Funding*

This research received no external funding.

#### *Acknowledgements*

The authors are highly thankful to the Chancellor, Sri Sai University, Palampur, H.P., for providing the lab facility.

## **REFERENCES**

- [1] Moslemizadeh A, Shadizadeh SR. A natural dye in water-based drilling fluids: Swelling inhibitive characteristic and side effects. *Petroleum*. 2017; 3(3):355–366.  
<https://doi.org/10.1016/j.petlm.2016.08.007>
- [2] Katheresan V, Kansedo J, Lau SY. Efficiency of various recent wastewater dye removal methods: A review. *Journal of Environmental Chemical Engineering*. 2018; 6(4):4676–4697.  
<https://doi.org/10.1016/j.jece.2018.06.060> Edgar KJ, Zhang H. Antibacterial modification of Lyocell fiber: A review. *Carbohydrate Polymers*. 2020; 250:116932.  
<https://doi.org/10.1016/j.carbpol.2020.116932>
- [3] Shibata Ates B, Koytepe S, Ulu A, Gurses C, Thakur VK. Chemistry, Structures, and Advanced Applications of Nanocomposites from Biorenewable Resources. *Chemical*

- Reviews. 2020; 120(17):9304–9362. <https://doi.org/10.1021/acs.chemrev.9b00553>
- [4] Serbanescu OS, Voicu SI, Thakur VK. Polysulfone functionalized membranes: Properties and challenges. *Materials Today Chemistry*. 2020; 17:100302. <https://doi.org/10.1016/j.mtchem.2020.100302>
- [5] Pandele AM, Comanici FE, Carp CA, Miculescu F, Voicu SI, Thakur VK, Serban BC. Synthesis and characterization of cellulose acetate-hydroxyapatite micro and nano composites membranes for water purification and biomedical applications. *Vacuum*. 2017; 146:599–605. <https://doi.org/10.1016/j.vacuum.2017.05.008>
- [6] Akpomie KG, Adegoke KA, Oyedotun KO, Ighalo JO, Amaku JF, Olisah C, Adeola AO, Iwuozor KO, Conradie J. Removal of bromophenol blue dye from water onto biomass, activated carbon, biochar, polymer, nanoparticle, and composite adsorbents. *Biomass Conversion and Biorefinery*. 2022. <https://doi.org/10.1007/s13399-022-03592-w>
- [7] Gayathiri E, Prakash P, Selvam K, Awasthi MK, Gobinath R, Karri RR, Ragunathan MG, Jayanthi J, Mani V, Poudineh MA, Chang SW, Ravindran B. Plant microbe based remediation approaches in dye removal: A review. *Bioengineered*. 2022; 13(3):7798–7828. <https://doi.org/10.1080/21655979.2022.2049100>
- [8] Aragaw TA, Bogale FM. Biomass-based adsorbents for removal of dyes from wastewater: a review. *Frontiers in Environmental Science*. 2021; 9. <https://doi.org/10.3389/fenvs.2021.764958>
- [9] Rana AK, Guleria S, Gupta VK, Thakur VK. Cellulosic pine needles-based biorefinery for a circular bioeconomy. *Bioresource Technology*. 2022; 367:128255. <https://doi.org/10.1016/j.biortech.2022.128255>
- [10] Rana AK. Green Approaches in the Valorization of Plant Wastes: Recent Insights and Future Directions. *Current Opinion in Green and Sustainable Chemistry*. 2022; 38:100696. <https://doi.org/10.1016/j.cogsc.2022.100696>
- [11] Haque ANMA, Sultana N, Sayem ASM, Smriti SA. Sustainable adsorbents from plant-derived agricultural wastes for anionic dye removal: a review. *Sustainability*. 2022; 14(17):11098. <https://doi.org/10.3390/su141711098>
- [12] Dallel R, Kesraoui A, Seffen M. Biosorption of cationic dye onto "Phragmites australis" fibers: Characterization and mechanism. *Journal of Environmental Chemical Engineering*. 2018; 6(6):7247–7256. <https://doi.org/10.1016/j.jece.2018.10.024>
- [13] Fan H, Ma Y, Wan J, Wang Y. Removal of gentian violet and rhodamine B using banyan aerial roots after modification and mechanism studies of differential adsorption behaviors. *Environmental Science and Pollution Research*. 2020; 27(9):9152–9166. <https://doi.org/10.1007/s11356-019-07024-7>

- [14] El-Sayed GO. Removal of methylene blue and crystal violet from aqueous solutions by palm kernel fiber. *Desalination*. 2011; 272(1–3):225–232. <https://doi.org/10.1016/j.desal.2011.01.025>
- [15] Singh M, Vajpayee M, Ledwani L. Eco-friendly surface modification of natural fibres to improve dye uptake using natural dyes and application of natural dyes in fabric finishing: A review. *Materials Today: Proceedings*. 2021; 43:2868–2871. <https://doi.org/10.1016/j.matpr.2021.01.078>
- [16] Mishra S, Cheng L, Maiti A. The utilization of agro-biomass/byproducts for effective bio-removal of dyes from dyeing wastewater: A comprehensive review. *Journal of Environmental Chemical Engineering*. 2021; 9(1):104901. <https://doi.org/10.1016/j.jece.2020.104901>
- [17] Rana AK, Gupta VK, Saini AK, Voicu SI, Abdellattifaand MH, Thakur VK. Water desalination using nanocelluloses/cellulose derivatives based membranes for sustainable future. *Desalination*. 2021; 520:115359. <https://doi.org/10.1016/j.desal.2021.115359>
- [18] Rana AK, Mishra YK, Gupta VK, Thakur VK. Sustainable materials in the removal of pesticides from contaminated water: Perspective on macro to nanoscale cellulose. *Science of The Total Environment*. 2021; 797:149129. <https://doi.org/10.1016/j.scitotenv.2021.149129>
- [19] Rana AK, Thakur VK. The bright side of cellulosic hibiscus sabdariffa fibres: towards sustainable materials from the macro-to nano-scale. *Materials Advances*. 2021; 2(15):4945–4965. <https://doi.org/10.1039/D1MA00429H>
- [20] Rana AK, Scarpa F, Thakur VK. Cellulose/polyaniline hybrid nanocomposites: Design, fabrication, and emerging multidimensional applications. *Industrial Crops and Products*. 2022; 187(Part A):115356. <https://doi.org/10.1016/j.indcrop.2022.115356>
- [21] Pushpa TB, Vijayaraghavan J, Basha SS, Sekaran V, Vijayaraghavan K, Jegan J. Investigation on removal of malachite green using EM based compost as adsorbent. *Ecotoxicology and Environmental Safety*. 2015; 118:177–182. <https://doi.org/10.1016/j.ecoenv.2015.04.033>
- [22] Tan IAW, Ahmad AL, Hameed BH. Enhancement of basic dye adsorption uptake from aqueous solutions using chemically modified oil palm shell activated carbon. *Colloids and Surfaces A: Physicochemical and Engineering Aspects*. 2008; 318(1–3):88–96. <https://doi.org/10.1016/j.colsurfa.2007.12.018>
- [23] Low LW, Teng TT, Ahmad A, Morad N, Wong YS. A novel pretreatment method of lignocellulosic material as adsorbent and kinetic study of dye waste adsorption. *Water, Air, & Soil Pollution*. 2011; 218(1):293–306. <https://doi.org/10.1007/s11270-010-0642-3>
- [24] Jawad AH, Rashid RA, Ishak MAM, Wilson LD. Adsorption of methylene blue onto activated carbon developed from biomass waste by H<sub>2</sub>SO<sub>4</sub> activation: kinetic, equilibrium and thermodynamic studies. *Desalination and Water Treatment*. 2016; 57(52):25194–25206. <https://doi.org/10.1080/19443994.2016.1144534>

- [25] Hamissa AMB, Lodi A, Seffen M, Finocchio E, Botter R, Converti A. Sorption of Cd (II) and Pb (II) from aqueous solutions onto Agave americana fibers. *Chemical Engineering Journal*. 2010; 159(1–3):67–74. <https://doi.org/10.1016/j.cej.2010.02.036>
- [26] Thimmiah BR, Nallathambi G. Development of high-performance filter from Agave americana fibre/polyacrylonitrile nanofibre membrane for Cd, Pb (II) and organic contaminants removal from aqueous solution. *Journal of Industrial Textiles*. 2022; 51(2\_suppl):2197S-2215S. <https://doi.org/10.1177/15280837221095203>
- [27] Ramana S, Tripathi AK, Kumar A, Dey P, Saha JK, Patra AK. Phytoremediation of soils contaminated with cadmium by Agave americana. *Journal of Natural Fibers*. 2021; 19(13):4984-4992. <https://doi.org/10.1080/15440478.2020.1870642>
- [28] Vivekanandan D, Sakthivel M. Fabrication and characterization of TiO<sub>2</sub> particulate filled agave Americana fiber-reinforced polyester resin composites. *Pigment & Resin Technology*. 2019; 48(6): 533-539. <https://doi.org/10.1108/PRT-08-2018-0079>
- [29] Hamissa AB, Brouers F, Ncibi MC, Seffen M. Kinetic modeling study on methylene blue sorption onto Agave americana fibers: fractal kinetics and regeneration studies. *Separation Science and Technology*. 2013; 48(18):2834–2842. <https://doi.org/10.1080/01496395.2013.809104>
- [30] Altinisik A, Seki Y, Ertas S, Akar E, Bozacı E, Seki Y. Evaluating of Agave americana fibers for biosorption of dye from aqueous solution. *Fibers and Polymers*. 2015; 16(2):370–377. <https://doi.org/10.1007/s12221-015-0370-9>
- [31] Hamissa AMB, Brouers F, Mahjoub B, Seffen M. Adsorption of textile dyes using Agave americana (L.) fibres: Equilibrium and kinetics modelling. *Adsorption Science & Technology*. 2007; 25(5):311–325. <https://doi.org/10.1260/026361707783432533>
- [32] Ben Hamissa AM, Ncibi MC, Mahjoub B, Seffen M. Biosorption of metal dye from aqueous solution onto Agave americana (L.) fibres. *International Journal of Environmental Science & Technology*. 2008; 5:501–508. <https://doi.org/10.1007/BF03326047>
- [33] Gupta VK, Agarwal S, Singh P, Pathania D. Acrylic acid grafted cellulosic Luffa cylindrical fiber for the removal of dye and metal ions. *Carbohydrate Polymers*. 2013; 98(1):1214–1221. <https://doi.org/10.1016/j.carbpol.2013.07.019>
- [34] Gupta VK, Pathania D, Sharma S, Agarwal S, Singh P. Remediation and recovery of methyl orange from aqueous solution onto acrylic acid grafted Ficus carica fiber: isotherms, kinetics and thermodynamics. *Journal of Molecular Liquids*. 2013; 177:325–334. <https://doi.org/10.1016/j.molliq.2012.10.007>
- [35] Sharma G, Naushad M, Pathania D, Mittal A, El-Desoky GE. Modification of Hibiscus cannabinus fiber by graft copolymerization: application for dye removal. *Desalination and Water Treatment*. 2015; 54(11):3114–3121. <https://doi.org/10.1080/19443994.2014.904822>

- [36] Pomicpic J, Dancel GC, Cabalar PJ, Madrid J. Methylene blue removal by poly (acrylic acid)-grafted pineapple leaf fiber/polyester nonwoven fabric adsorbent and its comparison with removal by gamma or electron beam irradiation. *Radiation Physics and Chemistry*. 2020; 172:108737. <https://doi.org/10.1016/j.radphyschem.2020.108737>
- [37] Hakam A, Rahman IA, Jamil MSM, Othaman R, Amin M, Lazim AM. Removal of methylene blue dye in aqueous solution by sorption on a bacterial-g-poly-(acrylic acid) polymer network hydrogel. *Sains Malaysiana*. 2015; 44(6):827–834.
- [38] Hong G, Cheng H, Meng Y, Lin J, Chen Z, Zhang S, Song W. Mussel-inspired polydopamine as a green, efficient, and stable platform to functionalize bamboo fiber with amino-terminated alkyl for high performance poly (butylene succinate) composites. *Polymers*. 2018; 10(4):461. <https://doi.org/10.3390/polym10040461>
- [39] Singha AS, Rana AK. Ce (IV) ion–initiated and microwave radiation–induced graft copolymerization of acrylic acid onto lignocellulosic fibers. *International Journal of Polymer Analysis and Characterization*. 2012; 17(1):72–84. <https://doi.org/10.1080/1023666X.2012.638753>
- [40] Mino G, Kaizerman S. A new method for the preparation of graft copolymers. *Polymerization initiated by ceric ion redox systems*. *Journal of Polymer Science*. 1958; 31(122):242–243. <https://doi.org/10.1002/pol.1958.1203112248>
- [41] Singha AS, Rana AK. Effect of graft copolymerization on mechanical, thermal, and chemical properties of grewia optiva/unsaturated polyester biocomposites. *Polymer Composites*. 2012; 33(8):1403–1414. <https://doi.org/10.1002/pc.22267>
- [42] Singha AS, Rana AK. Preparation and characterization of graft copolymerized Cannabis indica L. fiber-reinforced unsaturated polyester matrix-based biocomposites. *Journal of Reinforced Plastics and Composites*. 2012; 31(22):1538–1553. <https://doi.org/10.1177/0731684412442989>
- [43] Sharma S, Pardeep Singh D. Preparation, characterization and Cr (VI) adsorption behavior study of poly (acrylic acid) grafted Ficus carica bast fiber. *Advanced Materials Letters*. 2013; 4(4):271–276. <https://doi.org/10.5185/amlett.2012.8409>
- [44] Azari A, Kalantary RR, Ghanizadeh G, Kakavandi B, Farzadkia M, Ahmadi E. Iron–silver oxide nanoadsorbent synthesized by co-precipitation process for fluoride removal from aqueous solution and its adsorption mechanism. *RSC advances*. 2015; 5(106):87377–87391. <https://doi.org/10.1039/C5RA17595J>
- [45] Kumar P, Senthamil Selvi S, Govindaraju M. Seaweed-mediated biosynthesis of silver nanoparticles using Gracilaria corticata for its antifungal activity against Candida spp. *Applied Nanoscience*. 2013; 3(6):495–500. <https://doi.org/10.1007/s13204-012-0151-3>
- [46] Jiang G hua, Wang L, Chen T, Yu H jie, Wang J jun. Preparation and characterization of dendritic

- silver nanoparticles. *Journal of Materials Science*. 2005; 40(7):1681–1683.  
<https://doi.org/10.1007/s10853-005-0669-9>
- [47] Jyoti K, Baunthiyal M, Singh A. Characterization of silver nanoparticles synthesized using *Urtica dioica* Linn. leaves and their synergistic effects with antibiotics. *Journal of Radiation Research and Applied Sciences*. 2016; 9(3):217–227. <https://doi.org/10.1016/j.jrras.2015.10.002>
- [48] Prakash P, Gnanaprakasam P, Emmanuel R, Arokiyaraj S, Saravanan M. Green synthesis of silver nanoparticles from leaf extract of *Mimusops elengi*, Linn. for enhanced antibacterial activity against multi drug resistant clinical isolates. *Colloids and Surfaces B: Biointerfaces*. 2013; 108:255–259. <https://doi.org/10.1016/j.colsurfb.2013.03.017>
- [49] Zhang J, Liu K, Dai Z, Feng Y, Bao J, Mo X. Formation of novel assembled silver nanostructures from polyglycol solution. *Materials Chemistry and Physics*. 2006; 100(2–3):313–318.  
<https://doi.org/10.1016/j.matchemphys.2006.01.004>
- [50] Sarin V, Pant K. Removal of chromium from industrial waste by using eucalyptus bark. *Bioresource Technology*. 2006; 97(1):15–20. <https://doi.org/10.1016/j.biortech.2005.02.010>